Comparing Experimental Conditions for Efficient High Harmonic Generation

David Lloyd

Abstract

This document describes the rationale and theory behind a MATLAB program created to explore the optimal conditions for generating spectrally bright high-order harmonics.

Contents

February 22, 2018

1 Programme Outline

The program takes, as an input, values for the laser properties [pulse energy (E_0), duration (τ), spot size (w_0), and wavelength (λ)], in addition to the gas species and the harmonic photon energy one wishes to generate (γ_{in}). The program outputs two results, answering whether photons with energy in excess of (γ_{in}) are likely to be generated, and a 'figure of merit' (FoM) to express the likely spectral intensity into γ_{in} for the inputted parameters. Although "semi-analytic" expressions have been reported for the harmonic conversion efficiency [2], the simplified approach of using a 'figure of merit' allows, in principle, the different contributions to the overall harmonic flux (both macroscopic and microscopic) to be evaluated individually.

2 Version History

2.1 Version 1

- The figure of merit was (incorrectly) proportional to neutral population rather than the ion population.
- The FoM was proportional to number of emitters and hence harmonic field.
- An ADK ionization model was used.
- The length of focal volume was equal to the Rayleigh range.

2.2 Version 2 (current)

- The number of emitters is now proportional to ionization fraction (evaluated once the intensity is high enough for γ_{in} to be generated.
- The FoM is now proportional to the number of emitters squared, to reflect FoM proportionality with the harmonic intensity.
- The ionization fraction calculation has been changed to account for multiphoton ionization by using the Yudin and Ivanov model [1].
- The length of focal volume was set to half of the Rayleigh range of the fundamental.

3 Theory

3.1 In Brief

1. The user inputs: E_0, τ, w_0, λ, the gas species and γ_{in}.
2. The critical ionization fraction η_{c} is calculated using a plane wave approximation, see section 3.2 for the full expression.
3. The time dependence of the on-axis ionization fraction η is calculated using the theory of Yudin and Ivanov (YI) [1]. The *effective* peak laser intensity I_{eff} (by definition less than the vacuum peak intensity) occurs at a time when η first exceeds

η_c. It is assumed that no intensity greater than I_{eff} is accessed. The effective cut-off photon energy γ_{max} is found using the (single-atom) cut-off law and I_{eff}.

4. Each harmonic photon energy $\gamma < \gamma_{\text{max}}$ is associated with an ionization fraction. It is assumed that γ is generated at the instant of time that the intensity is high enough according to the cut-off law. Hence each γ is associated with the ionization fraction at the moment that the intensity is large enough for γ to be generated.

5. The phasematching pressure P_{m} is calculated (including the fundamental Gouy phase variation) for all $\gamma < \gamma_{\text{max}}$ using the matching η values, as defined in the previous step. See section 3.2 for the full expression.

6. The number of emitters (N), emitting at photon energy γ within the focal volume, is defined as the product of the number density (calculated from the phasematching pressure) and the volume of the focus $\frac{\pi^2 w_0^4}{2\lambda}$, where the longitudinal extent of the focal volume is defined as half the Rayleigh range.

7. The transmission $\bar{T}$ for photon energy γ is looked-up from a table downloaded from the CXRO database, adjusted for the phasematching pressure assuming Beer's law, and averaged over focal volume length.

8. The figure of merit for photon energy γ is given by:

$$FoM = \left(\frac{I_{\text{eff}}(\gamma)}{1 \times 10^{14}}\right)^3 \times \left(\frac{0.8}{\lambda}\right)^9 \times (\eta N)^2 \times \bar{T} \times w_0^{-2}. \tag{1}$$

The first term parameterises the dependence of the harmonic dipole strength on the fundamental intensity, with I_{eff} expressed in units of W/cm^2. The second term parameterises the dependence of the harmonic dipole on the fundamental wavelength, with λ expressed in units of microns. The third term represents the number of emitters in the focal volume. This term is squared to represent the coherent emission of all emitters contributing to the harmonic intensity. The fourth term accounts for reabsorption in the focal volume. The final w_0^{-2} term is included to obtain the correct spot size scaling as described in the work of Heyl [3].

3.2 In Detail

The numbering of subsections in this section correspond to the list numbering in section 3.1.

3.2.1 Input

The laser pulse is assumed to be a Gaussian in both spatial and temporal domains. The carrier envelope phase is fixed to 0. The inputted pulse duration is stated at its full width at half maximum. The inputted spot size is stated as its $1/e^2$ radius, such that Rayleigh range is given by: $z_{\text{r}} = \pi w_0^2/\lambda$. Hence the peak intensity is given by:

$$I = \frac{2E}{\tau \pi w_0^2}. \tag{2}$$

3.2.2 Critical Ionization

The critical ionization η_c is defined as the maximum ionization fraction in the medium which still allows phasematching to be achieved through adjusting the gas pressure. In other words, for ionization fractions $\eta > \eta_c$ phasematching is not possible. In the current GUI, η_c is found by solving for η when $\Delta k = 0$ in 1-D. Contributions to the dispersion from both the neutral gas and plasma are included but the geometric contribution to the dispersion (either Gouy or waveguide) is neglected yielding [4, 5]:

$$\eta_c = \left(1 + \frac{N_0 r_e \lambda^2}{2\pi\Delta n}\right)^{-1} \tag{3}$$

where N_0 is the number density at atmospheric pressure, r_e is the classical electron radius, and Δn is the difference between the refractive index evaluated at the fundamental wavelength (found using the Sellmeir equation for the gas species in question) and the harmonic wavelength (assumed to be one).

If instead the Gouy phase contribution to the dispersion is included a different expression is derived:

$$\eta_c = \frac{1 - \frac{\lambda^2 P_0}{(2\pi\Delta n)\pi w_0^2 P}}{1 + \frac{N_0 r_e \lambda^2}{2\pi\Delta n}} \tag{4}$$

where P_0 is atmospheric pressure. This expression reduces to equation 3 in the limit where $\frac{\lambda^2 P_0}{(2\pi\Delta n)\pi w_0^2 P} \ll 1$. Inspection of equation 4 reveals that the plane wave expression for η_c (equation 3) is always larger than the case where the Gouy phase dispersion is included (equation 4). In other words equation 3 overestimates η_c by a factor which depends on how tightly the fundamental is focused.

3.2.3 Ionization Fraction and Effective Peak Intensity.

The ionization fraction as a function of time η is found using the YI model for the inputted laser parameters and gas species [1]. It should be noted that the YI model accounts for both tunneling and multiphoton contributions to the ionization fraction, and is valid over a broader range of Keldysh parameters compared to the more common ADK model.

On the time scale of the laser pulse duration, η monotonically increases with time. Depending on the laser intensity and the gas species, it is possible for η to exceed η_c at some moment in time. At times later than this moment, phasematching is not possible.

It follows that it is possible to define an effective peak intensity I_{eff} for each of the two scenarios:

1. If η exceeds η_c at some moment prior to the pulse peak, then I_{eff} equals the intensity evaluated at the moment $\eta = \eta_c$.

2. Else if η is less than η_c at the peak of the laser pulse, then I_{eff} equals the theoretical peak intensity $2E/(\tau\pi w_0^2)$.

In the first case above, for peak intensities $I > I_{\text{eff}}$ phasematching is not possible. Hence we can derive an effective cut-off photon energy $\gamma_{\max}$ simply from the cut-off law evaluated with $I = I_{\text{eff}}$:

$$\gamma_{\max} = I_p + C I_{\text{eff}} \lambda^2 \tag{5}$$

where I_p is the ionization potential and C is a constant[1].

[1]When the units of $\gamma_{\max}$ and I_p are in eV, I_{eff} is in $W\text{cm}^{-2}$ and λ is in microns, then $C = 9.33 \times 10^{-13}$.

3.2.4 Mapping Ionization Fraction to Photon Energy

The highest harmonic photon energies will be localised to times where the ionization fraction is comparatively higher. To represent this, the user-desired photon energy γ_{in} can be related to the ionization fraction at the time the laser intensity just reaches a sufficient value for γ_{in} to be generated according to the cut-off law. Indeed, every $\gamma < \gamma_{\mathrm{max}}$ can be associated with an ionization fraction $\eta < \eta_{\mathrm{crit}}$, by the same rationale. For the subsequent calculation of the phasematching pressure, the variation of η with γ is included, yielding a phase-matching pressure which varies with photon energy.

3.2.5 Phasematching Pressure

The phasematching pressure is calculated by solving for P when $\Delta k = 0$, in 1-D, for the situation where dispersion comes from neutral gas, plasma and the Gouy phase [6]:

$$P_{\mathrm{m}} = \frac{P_0 \lambda^2}{2\pi^2 w_0^2 \Delta n (1 - \frac{\eta}{\eta_{\mathrm{c}}})}. \tag{6}$$

As noted in the same paper, equation 6 is valid for generation close to the driver focal plane, where the contribution to the dispersion from the intensity-dependent dipole phase is effectively cancelled out.

It can be seen that in the limit $\lim_{\eta \to \eta_{\mathrm{c}}} P_{\mathrm{m}} \to \infty$, hence it is not possible to phasematch photon energies $\gamma \geq \gamma_{\mathrm{max}}$.

3.2.6 Number of Emitters

The number density is derived from the phasematching pressure assuming the ideal gas law applies:

$$n_{\mathrm{d}} = \frac{P_m}{k_{\mathrm{B}} T} \tag{7}$$

where k_{B} is the Boltzmann constant and T is the temperature. As different phase-matching pressures apply for different photon energies, the number density is also a function of γ.

The focal volume is assumed to be cylindrical in shape, with a cross-sectional area of πw_0^2, with a longitudinal extent of $\frac{z_{\mathrm{r}}}{2} = \frac{\pi w_0^2}{2\lambda}$, and hence a total volume $V = \frac{\pi^2 w_0^4}{2\lambda}$.

The number of emitters is simply given by $N = n_{\mathrm{d}} \times V$.

3.2.7 Average Transmission

The transmission experienced by photons of energy γ traversing a distance z is given by:

$$T = \exp[-\alpha(\gamma) z] \tag{8}$$

where α is the (frequency dependent) attenuation coefficient, which is also dependent on the number density (n_{d}): $\alpha = \sigma n_{\mathrm{d}}$, where σ is the absorption cross-section. The species dependent absorption cross-section in the XUV can be obtained from the CXRO database.

For the figure of merit, we use the transmission averaged over the focal volume length ($\frac{z_\mathrm{r}}{2}$):

$$\begin{aligned}\bar{T}(\gamma_\mathrm{in}) &= \frac{2}{z_\mathrm{r}}\int_0^{\frac{z_\mathrm{r}}{2}} \exp[-\alpha(\gamma_\mathrm{in})z]dz \\ &= \frac{2}{\alpha z_\mathrm{r}}\Big\{1-\exp[-\frac{\alpha z_\mathrm{r}}{2}]\Big\}\end{aligned} \tag{9}$$

to reflect the assumption that the harmonic emission strength does not vary along the length of the focal volume.

3.2.8 Figure of Merit

The Figure of Merit is meant to represent a figure proportional to the spectral intensity evaluated at γ_in. It is given by:

$$FoM = \left(\frac{800}{\lambda}\right)^{5.5} \times (\eta N)^2 \times \bar{T}. \tag{10}$$

where the first factor relates to the single atom response, the second term is the number of emitters in the focal volume and the third term accounts for absorption in the generation region.

4 Discussion and Potential Improvements

There are some limitations to the FoM approach, as described above, for estimating the relative harmonic spectral intensity for a given set of conditions.

4.1 Recombination Dipole Matrix Element

The figure of merit shown in equation 10 fails to account for the gas species dependent 'scattering cross-section' of the returning electron wavepacket with the cation: experiments show that heavier gas species produce stronger harmonic emission. In the study performed by Gordon *et al.* it was shown that simulations relying on the Single Active Electron approximation yield an emission strength that does not change substantially for different noble gases [7]. Rather, 'many-electron effects' result in a variation of the species-dependent harmonic response. In the same paper the dipole acceleration was expressed as:

$$\langle \ddot{x} \rangle = -Z\langle \psi(t)|\frac{x}{r^3}|\psi(t)\rangle \tag{11}$$

where Z is the atomic number and $\psi(t)$ is the exact solution to the many-electron time dependent Schrödinger equation, which may be dependent on Z itself. Naïvely, we might assume that $\psi(t)$ is only weakly dependent on Z, and hence the harmonic intensity would be expected to scale with Z^2. However caution is required since both experiment and calculation [8] show that there is an additional order dependence (originating from the kinetic energy of the recolliding electron) that must also me taken into account. As yet, it is not clear how to include the Z dependence of the recombination dipole matrix element in the figure of merit.

On a related note, the figure of merit does not take into account 'structural' effects such as the Cooper minimum.

4.2 Transverse Source Size

The calculation assumes that the transverse source diameter of the harmonic is equal to the driver spot diameter ($2w_0$). Recent results suggest that harmonics of high order, which are also unaffected by absorption, have a constant source size [9]. It may also be the case that the very highest orders are confined to a region smaller than $2w_0$, where the intensity is high enough for those photon energies to be generated. An estimate of this order-dependent source size could, for instance, use the cut-off law to define the contour at which a high enough intensity is accessed to generate the user inputted photon energy.

4.3 More Complex Pulse Shapes

The calculation assumes that the pulse is unchirped and Gaussian shaped in both spatial and temporal dimensions. Different pulse envelope shapes and spectral phase functions could yield different behaviour. Further, the CEP is assumed to be zero. This parameter is unimportant for multi-cycle pulses, but is of key importance for few-cycle pulses.

5 Program Appearance

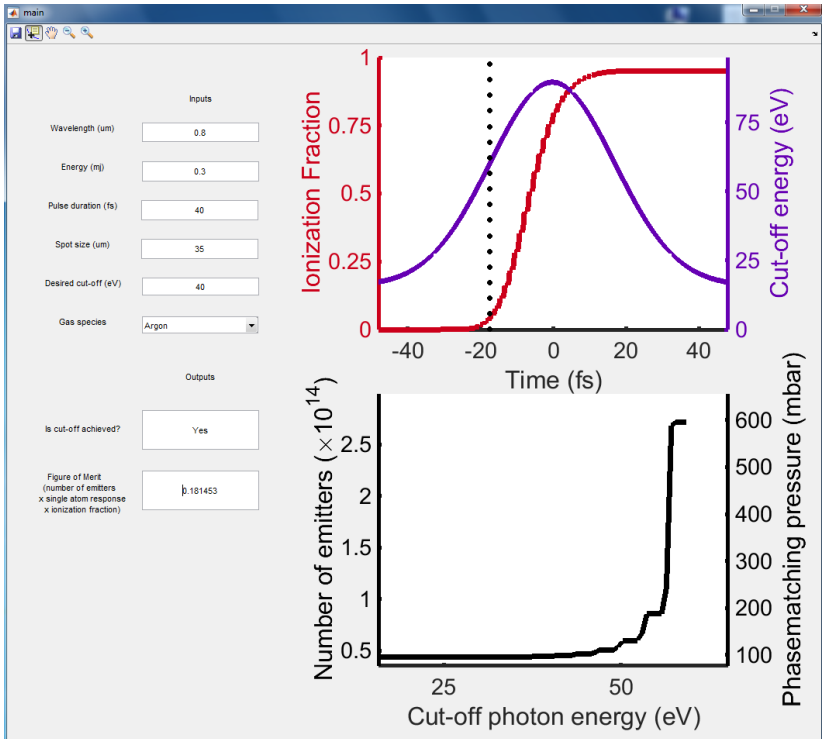

Figure 1: User interface of the program. Inputs are located on the top-left, outputs on the bottom right. The dotted black line in the upper figure denotes the time that η_c is achieved.

6 Technical Notes on the Program

The program was written in MATLAB. The executible file was created using the MATLAB Compiler. Either MATLAB Runtime must first be installed to run the executible file. MATLAB Runtime can be downloaded from `http://www.mathworks.com/products/compiler/mcr/index.html`.

References

[1] G. Yudin and M. Ivanov. 'Nonadiabatic Tunnel Ionization: Looking Inside a Laser Cycle', Physical Review A, 64, 013409 (2001)

[2] E. L. Falcao-Filho *et al.* 'Analytic Scaling Analysis of High Harmonic Generation Conversion Efficiency', Optics Express, 17(13) (2009).

[3] C. Heyl 'Scaling and Gating Attosecond Pulse Generation'. Doctoral thesis (2014). Available from `http://portal.research.lu.se/portal/files/3028441/4937902.pdf`.

[4] C. Durfee *et al.* 'Phase Matching of High-Oder Harmonics in Hollow Waveguides', Physical Review Letters, 83(11), (1999).

[5] Thomas A. Robinson. 'Quasi-Phase-Matching of High-Harmonic Generation'. DPhil thesis (2009). Available from `goo.gl/aIqvnD`.

[6] J. Rothhardt *et al.* 'Absorption-limited and Phase-matched High Harmonic Generation in the Tight Focussing Regime', New Journal of Physics, 16, 033022 (2014)

[7] A. Gordon *et al.* 'Role of Many-Electron Dynamics in High Harmonic Generation', Physical Review Letters, 96, 223902 (2006)

[8] J. Levesque *et al.* 'High Harmonic Generation and the Role of the Atomic Orbital Wave Functions', Physical Review Letters, 98, 183903 (2007)

[9] D. T. Lloyd *et al.* 'Gaussian-Schell Analysis of the Transverse Spatial Properties of High-harmonic Beams', Scientific Reports 6, 30504 (2016).